Large-scale absolute distance measurement with dual free-running all-polarization-maintaining femtosecond fiber lasers

Yuepeng Li (李跃鹏)[1], Yawen Cai (蔡娅雯)[2,*], Runmin Li (李润敏)[1], Haosen Shi (师浩森)[1], Haochen Tian (田昊晨)[1], Mingzhao He (赫明钊)[3], Youjian Song (宋有建)[1,], and Minglie Hu (胡明列)[1]**

[1]*Ultrafast Laser Laboratory, Key Laboratory of Opto-electronic Information Science and Technology of Ministry of Education, School of Precision Instruments and Opto-electronics Engineering, Tianjin University, Tianjin 300072, China*

[2]*Institute of Spacecraft System Engineering, China Academy of Space Technology, Beijing 100094, China*

[3]*National Institute of Metrology, Beijing 100029, China*

**Corresponding author: 739390293@qq.com; **corresponding author: yjsong@tju.edu.cn*

Received March 31, 2019; accepted May 23, 2019; posted online July 26, 2019

We demonstrate a robust femtosecond LIDAR setup by using two free-running environmentally stable all-polarization-maintaining nonlinear amplified loop mirror mode-locked fiber lasers. Based on the asynchronous optical sampling method, a ranging accuracy of ±2 μm within 65 m has been achieved, as tested in an 80-m-long underground optical tunnel. Through the Kalman filter in real-time data processing, the measurement accuracy can be maintained at a 200 Hz update rate. This setup provides a practical tool for various large-scale industrial and astronomical ranging applications.

OCIS codes: 120.0120, 140.4050, 320.7090.
doi: 10.3788/COL201917.091202.

High-accuracy large-scale length measurements are becoming more demanding in a variety of scientific and industrial fields. For large-scale structure fabrication and assembly, the three-dimensional (3D) coordinate metrology at length scales of 5 to 100 m has become a routine requirement[1]. Distributed synthetic aperture radar (SAR), which shows great potential in space-based surveillance, reconnaissance, and resource management, also relies on high-accuracy ranging and azimuth information. Typically, micrometer level ranging accuracy at a dozen meters of baseline is required[2]. Accuracy of conventional time-of-flight (TOF) LIDARS based on direct photoelectric detection of the retroreflected nanosecond laser pulses is restricted to millimeters due to limited response time of direct photo-detection[3]. Interferometric distance measuring techniques such as synthetic wavelength interference and multi-heterodyne interference, can also achieve absolute ranging[4,5]. However, for 10 μm level ranging accuracy, a sophisticated laser frequency stabilization apparatus is indispensable, which limits their applications in industrial fields and in space.

In recent years, absolute distance measurements based on femtosecond laser technology have become an active research field[6–11]. In particular, a dual-comb setup[12–15] draws great attention due to high resolution, high update rate, as well as dead-zone free measurement. Beam combination of two tightly phase-locked optical frequency combs with slightly different repetition rates naturally undergoes asynchronous optical sampling (ASOPS)[16], allowing precise timing determination for femtosecond laser pulses. Based on this principle, Coddington *et al.* achieved a ranging accuracy of 5 nm within a 1.5 m ambiguity range[12]. In a simplified setup without complex phase lock loops, Liu *et al.* obtained a ranging accuracy of 2 μm in 140 μs based on only two free-running low noise mode-locked femtosecond lasers[13]. A dual-wavelength passive mode-locked fiber laser that inherently emits dual pulse trains with an offset repetition rate was also used for absolute ranging, enabling a further simplified setup[14]. At the same time, the impact of the optical frequency comb design on dual-comb ranging precision has also been comprehensively investigated[17–19].

Compact and reliable femtosecond laser sources[20–23] are essential for practical femtosecond laser ranging applications. There has been rapid progress in this field. In 2014, an Er-doped femtosecond fiber laser based on a real saturable absorber (SA) mode locker was tested in aerospace[24]. The laser developed by South Korea operated well within a one-year in-orbit test. In order to avoid the low damage threshold and insufficient lifetime of a real SA, Germany tested an all-polarization-maintaining (PM) femtosecond fiber laser that is mode-locked by a nonlinear amplified loop mirror (NALM)[20], which acts as an artificial SA in space and showed its potential aerospace applications for optical clock comparison[25].

Despite the powerful all-PM NALM femtosecond laser technique and its potential for practical aerospace and industrial applications, its performance on absolute ranging has not been tested. In this Letter, we construct a simple and robust dual-comb LIDAR by employing two NALM mode-locked environmentally stable PM fiber lasers with ~2 kHz offset repetition rate as laser sources. The absolute

distance is measured through an ASOPS-based TOF method. A ranging accuracy of ±2 μm within 65 m is realized. A high update rate is maintained by using Kalman filtering for real-time data processing.

The NALM mode-locked fiber laser used for absolute ranging contains a fiber loop and a linear arm, as schematically shown in Fig. 1. The counter-propagating pulses in the fiber loop obtain asymmetrical gain, hence differential nonlinear phase. They combine at the linear arm, and the interference between two pulses introduces an intensity-dependent response, serving as a fast SA. A Faraday rotator and a quarter waveplate (QWP1) work as a nonreciprocal phase shifter, introducing an additional phase bias, which contributes to self-started mode-locking[20]. Two output ports with tunable output power are obtained through QWP2. In this system, port 1 is used for distance measurement, while port 2 is used for monitoring.

Two home-built all-PM NALM mode-locked fiber lasers with ∼2 kHz repetition rate difference were used for the dual-comb ranging system. The optical spectra of the two lasers are shown in the inset of Fig. 1, and the output parameters are listed in Table 1.

The principle of ASOPS-based TOF measurement is shown in Fig. 2[17]. The pulse train emitted from the signal laser (SL) with a repetition rate of f_r is partly reflected by a reference mirror, and the transmitted part is then reflected by a target mirror. The collected reference-reflected and

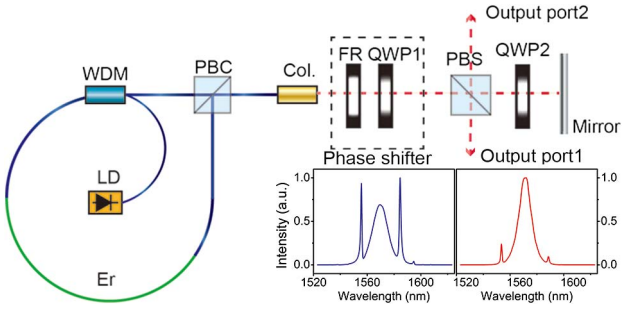

Fig. 1. Configuration of all-PM NALM mode-locked fiber laser. WDM, 980/1550 nm wavelength division multiplexer; PBC, polarization beam coupler; Col., collimator; FR, Faraday rotator; QWP, quarter waveplate. The FR and QWP form the nonreciprocal phase shifter. Optical spectra of two mode-locked lasers. Blue line, laser 1; red line, laser 2.

Table 1. Output Parameters of Two Lasers

Parameters	Laser 1	Laser 2
Pump power	218.7 mW	220.3 mW
Output1 power	6.20 mW	7.69 mW
Output2 power	15.58 mW	14.66 mW
Repetition rate	80.267 MHz	80.269 MHz
λ_c	1569.4 nm	1571.8 nm
FWHM	13.2 nm	11.8 nm

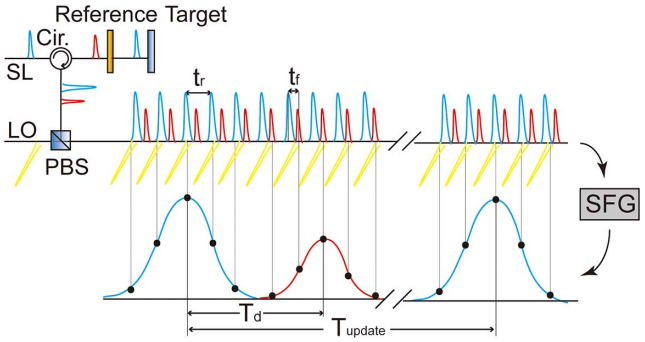

Fig. 2. Working principle of ASOPS. Two laser sources that have slightly different repetition frequency rates (f_r and $f_r + \Delta f_r$) are used. Every period T_{update}, the LO will take a complete sampling signal of the SL pulse via sum-frequency generation (SFG).

target-reflected pulse trains are combined with the pulse train from a local oscillator (LO), which has a repetition rate of $f_r + \Delta f_r$. The repetition rate difference between the SL and LO causes a walk-off between these pulse trains, ensuring that the LO pulse train takes a sample of the reflected SL pulse train over many repetition periods (t_r). In other words, LO pulses walk through the reflected SL pulses with a step of

$$\Delta t = \frac{1}{f_r} - \frac{1}{f_r + \Delta f_r} \approx \frac{\Delta f_r}{f_r^2} \tag{1}$$

at each repetition period. A full scan of the LO pulses across the reflected SL pulses is completed every

$$T_{\text{update}} = \frac{1}{\Delta f_r}. \tag{2}$$

Equivalently, the SL pulses are temporally stretched by a factor of N, where

$$N = \frac{t_r}{\Delta t} = \frac{f_r}{\Delta f_r}. \tag{3}$$

To this end, the time interval of reflected reference and target pulses t_f can be obtained through fast data acquisition electronics. The target distance is simply

$$L = \frac{c}{2n_g} \cdot t_f = \frac{c}{2n_g} \cdot \left(\frac{T_d}{N} + mt_r\right), \tag{4}$$

where n_g is the group refractive index of air, T_d is the obtained time interval between the adjacent target and reference pulses in the stretched time window, and m is an integer that accounts for ranging ambiguity. Instead of directly measuring N, we determine the distance by using

$$L = \frac{c}{2n_g} \cdot \frac{1}{f_r} \cdot \left(\frac{T_{\text{tar}} - T_{\text{ref1}}}{T_{\text{ref2}} - T_{\text{ref1}}} + m\right), \tag{5}$$

where T_{tar} is the timing of the target pulse, and T_{ref1} and T_{ref2} represent timing of two successive reference pulses, all

measured in the stretched time window. There is a ~0.5 mm dead zone caused by the overlap of the reference pulse and target pulse in the vicinity of each integer non-ambiguous range. This small dead zone can be avoided by detecting the reference and measurement pulses separately[7].

The experimental setup of the femtosecond LIDAR system is shown in Fig. 3. The SL and LO in Fig. 3 are as aforementioned free-running all-PM NALM fiber lasers. For compactness and robustness, the free-space outputs from port 1 of the two lasers are coupled into fiber through a space coupler, which contains an isolator, a half-waveplate, and a collimator.

A reference mirror, telescope, and target mirror are placed after port 2 of a fiber circulator. Note that the 4% Fresnel reflection from the end face of a ferrule connector/physical contact (FC/PC) connector acts as the reference mirror. A telescope (Thorlabs, C80APC-C) with adjustable focus length is used to collimate the beam for long-distance ranging. The target mirror is a hollow retroreflector installed at an 80 m granite rail at the National Institute of Metrology, China (NIM). The reflected pulses of the SL laser are combined with the LO pulses through a polarization beam splitter (PBS). Then, the reflected SL pulses are sampled by the LO via sum frequency generation in a type-II periodically poled $KTiOPO_4$ (PPKTP) crystal, thus completing the ASOPS process. Finally, the intensity cross-correlation trace is detected by a low noise avalanche photo-detector (Thorlabs, APD120 A). After a low pass filter (30 MHz), the trace is digitized and stored by a data acquisition card (NI PXIe-5122). The repetition rate of the SL pulse train is real-time monitored by a 12 bit frequency counter (Agilent, 53220 A) at 1 s gate time, which is used as an external signal clock for the data acquisition card.

The absolute distance between the reference and target mirror is retrieved from the time interval between adjacent reference and target pulses in a stretched window, which is obtained by extracting the interval between peaks of the Gaussian fitted cross-correlation trace. The meter level non-ambiguity range can be resolved by non-ambiguity range extension approaches[12,26], or simply by a number of coarse measurement methods. Here, we determine m by gauge readings on the granite rail. The absolute distance measurement results of this LIDAR system are compared with the 80 m laser comparator at NIM, as shown in Fig. 4(a). The residuals and standard deviations of the ranging results are depicted in Fig. 4(b). The absolute values of the residuals are within 2 μm with standard deviations less than 4 μm over the full 65 m measurement range at an averaging time of 500 ms. The Allan deviation of the results at two selected positions of 30

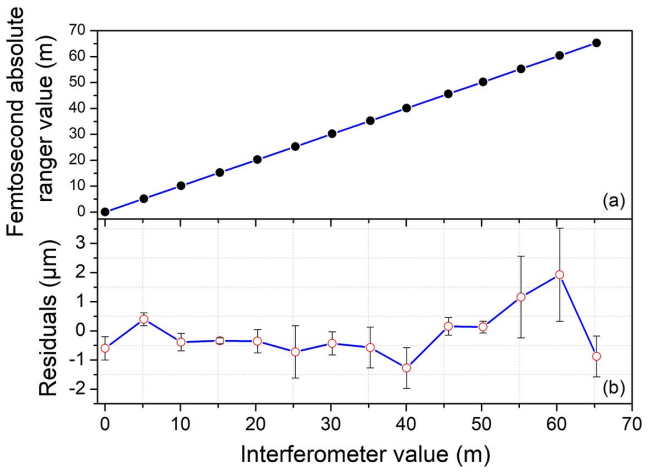

Fig. 4. (a) Absolute distance measurement results of the femtosecond absolute ranger compared with the standard interferometers. (b) Residuals of measured distance versus truth data from standard interferometers at the NIM. The averaging period for the TOF measurement is 500 ms.

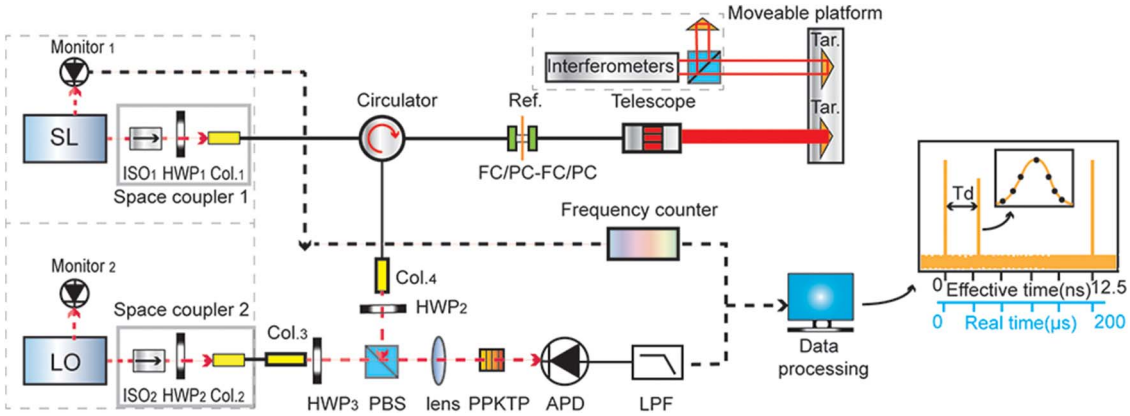

Fig. 3. Experimental setup of the robust LIDAR system. Two free-running all-PM lasers with slightly different repetition rates (~80.267 MHz, ~82.269 MHz) are used as the laser sources. An FC/PC connector having 4% Fresnel reflection at the surface and a hollow retroreflector are used as the reference and target mirror, respectively. The absolute distance between the reference and target mirrors is obtained through optical intensity cross-correlation between the reflected SL and LO pulses. Note that the telescope is focal length adjustable. SL, single laser; LO, local oscillator; ISO, isolator; HWP, half-waveplate; Col., collimator; Ref., reference mirror; Tar., target mirror; PBS, polarization beam splitter; PPKTP, periodically poled $KTiOPO_4$; APD, avalanche photo-detector; LPF, low pass filter.

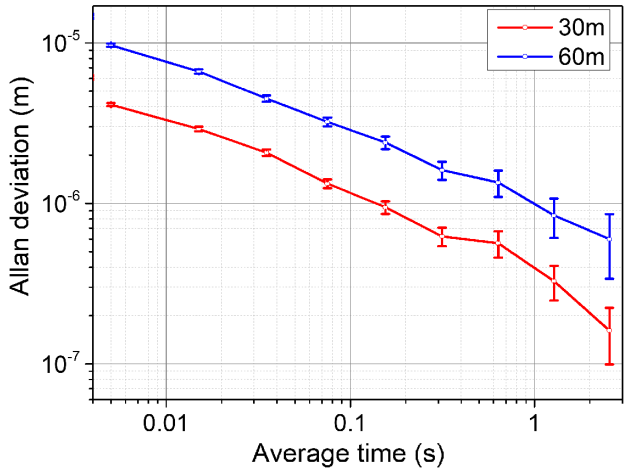

Fig. 5. Allan deviations at absolute distances of 30 and 60 m. The measurement accuracy increases with the increase of averaging time and reaches less than 1 μm at 1 s averaging time.

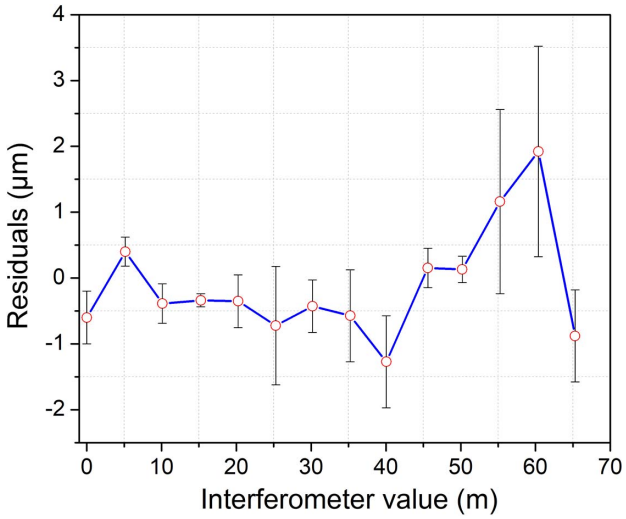

Fig. 6. Residuals of measured distance after the Kalman filter compared with the standard interferometers. The residuals and deviations are less than 3 μm, while the update rate is 200 Hz.

and 60 m are shown in Fig. 5. At the minimum acquisition time of 5 ms (set by the data processing module), the standard deviations are 4.1 μm at 30 m and 9.6 μm at 60 m, respectively. The precision drops below 1 μm when the averaging time is increased to 1 s.

Allan deviation in Fig. 5 indicates a white noise timing fluctuation during TOF determination. A number of advanced data processing techniques can be used to reduce white noise besides simple multiple averaging, which secures a high measurement precision by sacrificing the update rate. Here, we utilized the Kalman filter[27] to reduce the measurement precision loss introduced by the stochastic process and maintain a high measurement update rate. Kalman filtering has been frequently used to filter noisy signals in dynamic systems. Here, the procedure of Kalman filtering establishes a space model to calculate the optimal state estimation of the absolute distance measurement results. The specific procedure of applying the Kalman filtering algorithm for processing distance signals obtained by the dual-comb absolute ranging system can be found in our earlier publication[28]. The acquired distance data are processed by Kalman filtering during measurement, and the results are depicted in Fig. 6. The residuals and standard deviation are of the same level as those in Fig. 4, while a 200 Hz update rate is maintained.

In conclusion, a robust dual-comb LIDAR system based on all-PM femtosecond fiber lasers is demonstrated. Large-scale absolute distance measurement is conducted at an 80 m granite rail at the NIM. The measurement residuals are less than 2 μm, and deviations are less than 6 μm with 500 ms averaging time over 65 m distance. Through the Kalman filter in data processing, the update rate increases to 200 Hz, while the micrometer accuracy is maintained. The all-PM fiber, high accuracy, and high update rate femtosecond LIDAR system shows great promise for various space-based large-scale measurement applications, such as distributed SAR remote sensing, gravitational wave detection, and a satellite formation flying-based astronomical telescope.

This work was supported by the Natural Science Foundation of Tianjin (No. 18JCYBJC16900) and the National Natural Science Foundation of China (NSFC) (Nos. 61675150, 61827821, and 61535009).

References

1. W. T. Estler, K. L. Edmundson, G. N. Peggs, and D. H. Parker, CIRP Ann. **51**, 587 (2002).
2. G. Krieger and A. Moreira, in *IEEE Geoscience & Remote Sensing Symposium* (2010), p. 993.
3. J. Yun, C. Gao, S. Zhu, C. Sun, and L. Niu, Chin. Opt. Lett. **10**, 121402 (2012).
4. X. Wu, H. Wei, H. Zhang, and J. Zhang, Appl. Opt. **52**, 2042 (2013).
5. O. P. Lay, S. Dubovitsky, R. D. Peters, and W. Steier, Opt. Lett. **28**, 890 (2003).
6. J. Ye, Opt. Lett. **29**, 1153 (2004).
7. J. Lee, S. Han, K. Lee, and Y. J. Kim, Meas. Sci. Technol. **24**, 045201 (2013).
8. Y. S. Jang and S. W. Kim, Nanomanuf. Metrol. **1**, 131 (2018).
9. X. Zhao, X. Qu, F. Zhang, and G. Tang, Opt. Lett. **43**, 807 (2018).
10. G. Wu, M. Takahashi, H. Inaba, and K. Minoshima, Opt. Lett. **38**, 2140 (2013).
11. H. Zhang, H. Wei, X. Wu, and Y. Li, IEEE Photon. J. **7**, 6801508 (2015).
12. I. Coddington, W. C. Swann, L. Nenadovic, and N. R. Newbury, Nat. Photonics **3**, 351 (2009).
13. T. A. Liu, N. R. Newbury, and I. Coddington, Opt. Express **19**, 18501 (2011).
14. B. Lin, X. Zhao, M. He, and Y. Pan, IEEE Photon. J. **9**, 7106508 (2017).
15. Z. Zhu, G. Xu, K. Ni, Q. Zhou, and G. Wu, Opt. Express **26**, 5747 (2018).
16. H. Zhang, H. Wei, X. Wu, H. Yang, and Y. Li, Opt. Express **22**, 6597 (2014).
17. H. Shi, Y. Song, F. Liang, L. Xu, M. Hu, and C. Wang, Opt. Express **23**, 14057 (2015).

18. Y. Li, J. Shi, Y. Wang, R. Ji, D. Liu, and W. Zhou, Meas. Sci. Technol. **28**, 075201 (2017).
19. G. Wu, Q. Zhou, L. Shen, K. Ni, X. Zeng, and Y. Li, Appl. Phys. Express **7**, 106602 (2014).
20. W. Hänsel, H. Hoogland, M. Giunta, T. Steinmetz, and R. Doubek, Appl. Phys. B **123**, 41 (2017).
21. W. Dai, Y. Song, B. Xu, A. Martinez, S. Yamashita, and M. Hu, Chin. Opt. Lett. **12**, 123502 (2014).
22. A. Nady, M. H. M. Ahmed, A. A. Latiff, C. H. Raymond Ooi, and S. W. Harun, Chin. Opt. Lett. **15**, 100602 (2017).
23. X. Wu, L. Yang, H. Zhang, H. Yang, H. Wei, and Y. Li, Appl. Opt. **54**, 1681 (2015).
24. J. Lee, K. Lee, Y. S. Jang, H. Jang, S. Han, and S. H. Lee, Sci. Rep. **4**, 5134 (2014).
25. M. Lezius, T. Wilken, C. Deutsch, M. Giunta, O. Mandel, and A. Thaller, Optica **3**, 1381 (2016).
26. H. Zhang, H. Wei, X. Wu, H. Yang, and Y. Li, Meas. Sci. Technol. **25**, 125201 (2014).
27. P. Zarchan and H. Muso, *Fundamentals of Kalman Filtering: A Practical Approach* (American Institute of Aeronautics and Astronautics, 2000).
28. J. Yu, H. Shi, Y. Song, H. Cao, M. Hu, and C. Wang, Chin. J. Lasers **44**, 0610001 (2017).